
Article:
Blümke, A., Sode, B., Ellinger, D. et al. (1 more author) (2015) Reduced susceptibility to Fusarium head blight in Brachypodium distachyon through priming with the Fusarium mycotoxin deoxynivalenol. Molecular Plant Pathology, 16 (5). pp. 472-483. ISSN 1464-6722

https://doi.org/10.1111/mpp.12203

Figure 1. Numeric scoring system for rating the disease severity of *F. graminearum*-infected *B. distachyon* spikelets.
(A) Uninfected floret, disease score 0.0.
(B) Weak infection of a floret, only one small, restricted necrosis (N) visible on the caryopsis or the rachilla, disease score: 0.1.
(C) More than one necrotic lesion and/or lesion(s) covering a maximum of 50 % of the infected floret, disease score: 0.5.
(D) Extended necrosis covering more than half of the floret, highest disease score of 1.0. For each spikelet, single florets were rated 14 d post-inoculation with *F. graminearum* strains and the score was calculated as indicated in the formula. L, lemma. Scale bar = 2 mm.

Numeric scoring system for rating the disease severity of F. graminearum-infected B. distachyon spikelets.
156x77mm (300 x 300 DPI)

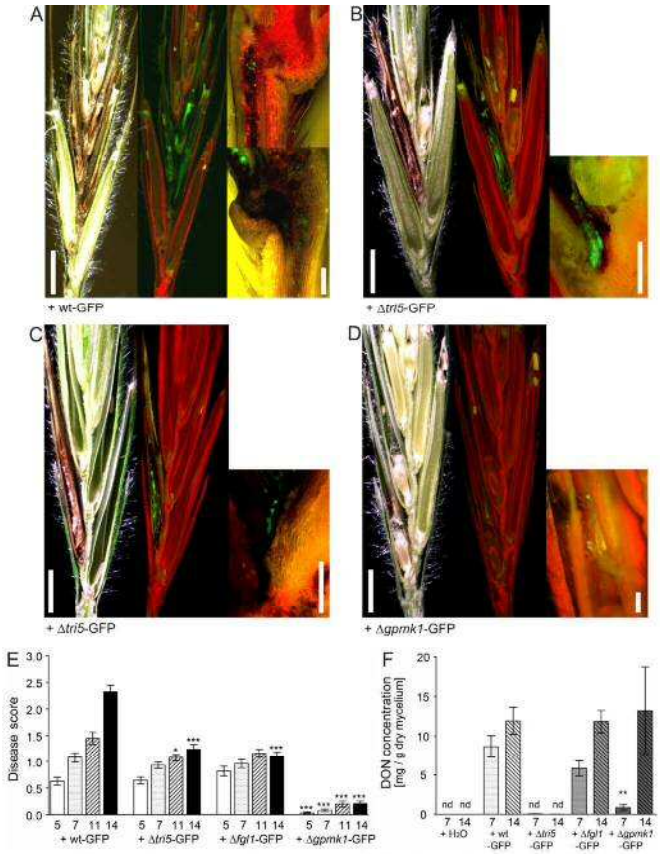

Figure 2. Disease phenotype and DON accumulation in *B. distachyon* spikelets after *F. graminearum* infection.
(A-D) Micrographs of longitudinal sectioned spikelets 14 d post-inoculation (dpi) with the GFP-tagged *F. graminearum* strains: (A) wild-type wt-GFP, (B) DON-deficient disruption mutant Δ*tri5*-GFP, (C) lipase-deficient disruption mutant Δ*flg1*-GFP, and (D) MAP kinase-deficient disruption mutant Δ*gpmk1*-GFP. Left panels: images of spikelet sections with bright field illumination to visualize necrotic tissue; mid-panels: images of same sections as in left panels, but with epi-fluorescent illumination to visualize GFP-emitting fungal hyphae; and right panels: magnification of the rachilla of inoculated florets with epi-fluorescent illumination. Scale bars for left and mid-panels = 2 mm, for right panels = 0.2 mm.
(E) Disease score of infected spikelets 5, 7, 11, and 14 dpi with GFP-tagged *F. graminearum* strains as indicated. $*p < 0.05$, $***p < 0.005$ Dunnett's test. Error bars represent ± SEM, and $n \geq 12$.
(F) DON concentration of infected spikelet tissue 7 and 14 dpi with GFP-tagged *F. graminearum* strains as indicated. Water-inoculated spikelets served as control. $**p < 0.01$ Dunnett's test. Error bars represent ± SEM , and $n = 3$. nd, not detectable.

Disease phenotype and DON accumulation in B. distachyon spikelets after F. graminearum infection.
142x255mm (300 x 300 DPI)

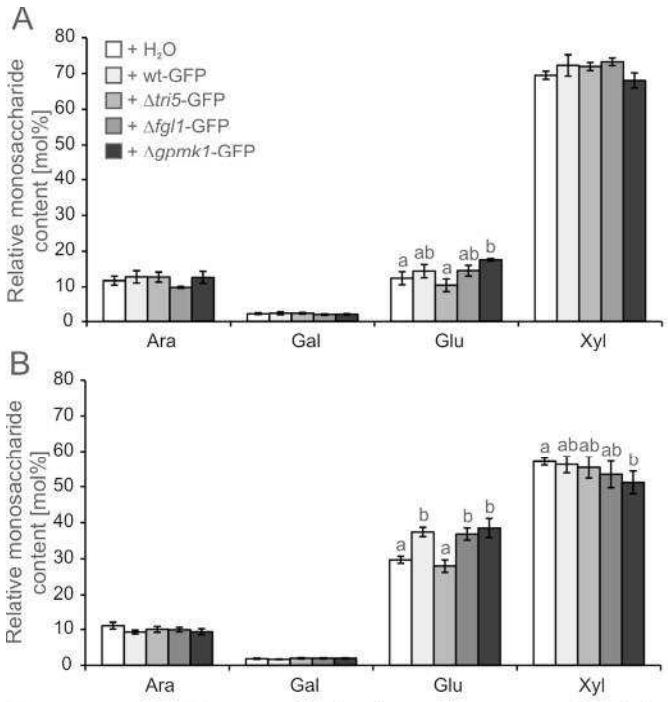

Figure 3. Non-cellulosic monosaccharide composition of *B. distachyon* spikelets after *F. graminearum* infection.
Cell wall extracts from infected spikelets at **(A)** 7 d post-inoculation (dpi) and **(B)** 14 dpi with the GFP-tagged *F. graminearum* strains wt-GFP, Δ*tri5*-GFP, Δ*flg1*-GFP, and Δ*gpmk1*-GFP were used. Water-inoculated spikelets served as control. Non-cellulosic monosaccharide composition determined by HPAEC-PAD (high-performance anion exchange chromatography with pulsed amperometric detection). a,b: $p < 0.05$ Dunnett's test. Error bars represent ± SEM , and $n = 3$. Ara, L-arabinose; Gal, D-galactose; Glu, D–glucose; Xyl, D-xylose.

Non-cellulosic monosaccharide composition of B. distachyon spikelets after F. graminearum infection.
87x156mm (300 x 300 DPI)

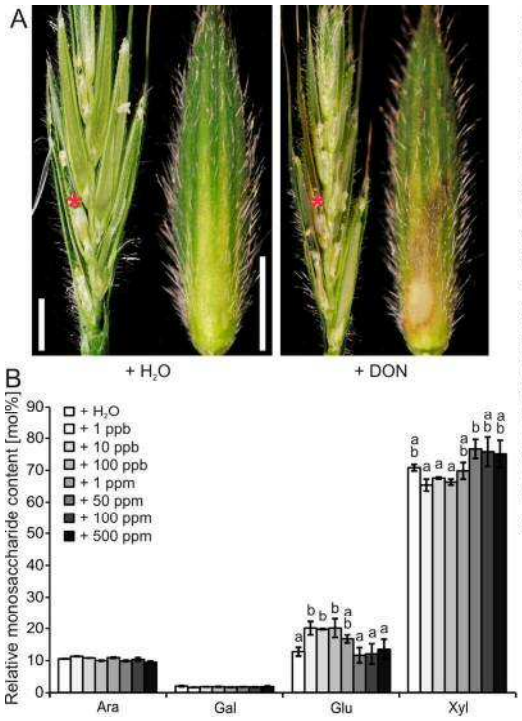

Figure 4. DON-induced cell wall changes in *B. distachyon* spikelets.
A single floret of a spikelet was point-inoculated with DON solutions at concentrations ranging from 1 ppb to 500 ppm. Spikelets inoculated with water and *F. graminearum* strain wt-GFP served as control. **(A)** Longitudinal spikelet section (left part of each panel) and isolated lemma (right part of each panel) of an inoculated floret 7 d after water and DON application at a concentration of 500 ppm. Red asterisk indicates point-inoculated floret. Scale bars = 2 mm. **(B)** Non-cellulosic monosaccharide composition of cell wall extracts from spikelets treated with DON at indicated concentrations 7 d after application. a,b: $p < 0.05$ Dunnett's test. Error bars represent ± SEM, and $n = 3$. Ara, L-arabinose; Gal, D-galactose; Glu, D–glucose; Xyl, D-xylose.

DON-induced cell wall changes in B. distachyon spikelets.
162x115mm (300 x 300 DPI)

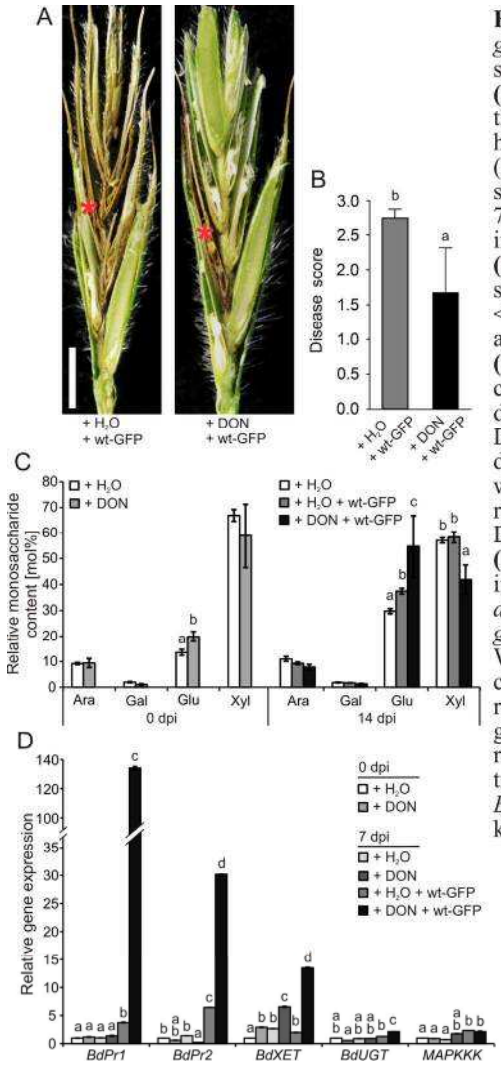

Figure 5. DON-induced resistance to *F. graminearum* colonization of *B. distachyon* spikelets.
(A) Longitudinal section of spikelets infected with the wild-type *F. graminearum* strain wt-GFP to highlight disease phenotype 14 d post-inoculation (dpi). Spikelets were pretreated by spraying a DON solution (concentration: 1 ppm) and water as control 7 d before *F. graminearum* inoculation. Red asterisk indicates point-inoculated floret. Scale bar = 2 mm.
(B) Disease score of water- and DON-pretreated spikelets 14 dpi with *F. graminearum* wt-GFP. a,b: $p < 0.05$ Dunnett's test. Error bars represent ± SEM, and $n \geq 12$.
(C) Non-cellulosic monosaccharide composition of cell wall extracts from spikelets 7 d after spraying (0 dpi, time-point of *F. graminearum* inoculation) of DON or water as control (as described in (A)) and 14 dpi of the pretreated spikelets with *F. graminearum* wt-GFP. a,b,c: $p < 0.05$ Dunnett's test. Error bars represent ± SEM , and $n = 3$. Ara, L-arabinose; Gal, D-galactose; Glu, D–glucose; Xyl, D-xylose.
(D) Expression analysis of pathogen- and DON-inducible genes in DON- and water-pretreated *B. distachyon* spikelets at the time-point of *F. graminearum* wt-GFP inoculation (0 dpi) and 7 dpi. Water-sprayed, unchallenged spikelets served as control. a,b,c,d: $p < 0.05$ Dunnett's test. Error bars represent ± SEM , and $n = 3$. A repeat experiment gave similar results. *BdPR1.1*/*BdPR2*, pathogenesis related genes; *BdXET*, xyloglucan xyloglucosyl transferase; *BdUGT*, UDP-glycosyltransferase; *BdMAPKKK*, mitogen-activated protein kinase kinase kinase.

DON-induced resistance to F. graminearum colonization of B. distachyon spikelets.
172x181mm (300 x 300 DPI)

Reduced susceptibility to Fusarium head blight in *Brachypodium distachyon* through priming with the *Fusarium* mycotoxin deoxynivalenol

Antje Blümke, Björn Sode, Dorothea Ellinger and Christian A. Voigt*

Phytopathology and Biochemistry, Biocenter Klein Flottbek, University of Hamburg,

Ohnhorststr. 18, 22609 Hamburg, Germany

RUNNING TITLE: **DON priming in pathogen resistance**

*Corresponding author

Contact:

University of Hamburg, Biocenter Klein Flottbek

Ohnhorststr. 18, 22609 Hamburg, Germany

E-mail: christian.voigt@uni-hamburg.de

Telephone: ++49-40-42816-331

Fax: ++49-40-42816-631

Word count:

Summary	224
Introduction	1,153
Results	2,010
Discussion	1,568
Experimental Procedures	1,202
Acknowledgements	28
Figure Legends	751
Total	**6,936**

SUMMARY

The fungal cereal-pathogen *Fusarium graminearum* produces deoxynivalenol (DON) during infection. The mycotoxin DON is associated with Fusarium head blight (FHB), a disease that can cause vast grain losses.

Whilst investigating the suitability of *Brachypodium distachyon* as a model for spreading resistance to *F. graminearum*, we unexpectedly discovered that a DON pretreatment of spikelets could reduce susceptibility to FHB in this model grass.

We started to analyze cell wall changes in spikelets after infection with *F. graminearum* wild-type and defined mutants: the DON-deficient Δ*tri5* mutant and the DON-producing lipase-disruption mutant Δ*fgl1*, both infecting only directly inoculated florets, and the MAP kinase disruption mutant Δ*gpmk1* with strongly decreased virulence but intact DON production. At 14 d post-inoculation, the glucose amount in the non-cellulosic cell wall fraction was only increased in spikelets infected with the DON-producing strains wild-type, Δ*fgl1*, and Δ*gpmk1*. Hence, we tested for DON-induced cell wall changes in *B. distachyon*, which were most prominent at DON concentrations ranging from 1 ppb to 100 ppb. To test an involvement of DON in defense priming, we pretreated spikelets with DON at a concentration of 1 ppm prior *F. graminearum* wild-type infection, which significantly reduced FHB disease symptoms. Analysis of cell wall composition and plant defense-related gene expression after DON pretreatment and fungal infection suggests that DON-induced priming of the spikelet tissue contributed to reduced susceptibility to FHB.

KEYWORDS

Brachypodium distachyon, cell wall, deoxynivalenol, *Fusarium graminearum*, fungal resistance, mycotoxin, plant defense

.

INTRODUCTION

Based on its phylogeny and morphology, the small annual grass *Brachypodium distachyon* has emerged as a model system for the investigation of Triticeae (Catalán *et al.*, 1995, Vogel & Bragg, 2009, Vogel *et al.*, 2006). Among this tribe of Poaceae, wheat (*Triticum aestivum*) has the highest agronomic importance as it was the third most-produced cereal after maize (*Zea mays*) and rice (*Oryza sativa*) in 2012 according to the FAO statistics (Food and Agriculture Organization of the United Nations, 2014, http://faostat3.fao.org/faostat-gateway/go/to/download/Q/QC/E). Therefore, yield losses have a direct impact on the world food production. Pathogens represent a major cause of yield losses in wheat. Under weather conditions favoring an epidemic outbreak, the fungal crop disease Fusarium head blight (FHB) alone can account for over 40% yield loss on wheat, even in countries with a high degree of mechanization and surveillance systems available like in the US (Cowger & Sutton, 2005). The main causative fungal species of FHB is *Fusarium graminearum*. In recent years, an increasing spread *F. graminearum* further raised its importance for agriculture (Chakraborty & Newton, 2011, Madgwick *et al*., 2011). New challenges might emerge from climate change. Changing rainfall patterns already increased FHB dramatically in the Punjab region of India in 2005 (Duveiller *et al*., 2007). The occurrence of extreme weather situations would decrease prediction efficiency of existing agricultural surveillance systems and favor FHB outbreaks. FHB is characterized by a bleaching of the spike. Due to sterile florets and shriveled, not properly developed kernels, *F. graminearum*-based FHB is associated with severe losses in yield and reduction in baking and seed quality (McMullen *et al*., 1997, Pirgozliev, 2003). In addition to yield losses, mycotoxins produced by

F. graminearum are a threat for human and animal health. Mycotoxins like the potent estrogenic metabolite zearalenone (Peraica *et al.*, 1999) and the trichothecene deoxynivalenol (DON) can contaminate the remaining grain. DON can depress the immune system and inhibits eukaryotic protein biosynthesis through binding to the 60S ribosomal subunit of eukaryotes (Kimura *et al*., 1998, Rocha *et al*., 2005). In plants, DON accumulation induces disease symptoms including necrosis, chlorosis, and wilting (Cutler, 1988). Due to its importance in agriculture, efforts are being made to enhance the resistance of wheat to *F. graminearum* and FHB. The application of biotechnological methods to reduce susceptibility to *F. graminearum* is more complicated compared to many other crops. A main reason is the limited genetic access of wheat. The large and complex genome structure in combination with low transformation efficiency restricts the identification of putative targets for increased plant resistance and their direct modification. Therefore, most strategies follow conventional breeding strategies using wheat cultivars with observed reduced FHB disease symptoms like Sumai 3 (del Blanco *et al.*, 2003). However, despite this breeding efforts, most commercial available wheat cultivars used for food production are still susceptible to *F. graminearum* (Buerstmayr *et al.*, 2009). To overcome restrictions in the analysis of the pathosystem *F. graminearum* – wheat, *B. distachyon* was identified as an appropriate plant for genetic and molecular analysis. Peraldi *et al*. (2011) showed that *F. graminearum* can infect the spikelet of *B. distachyon*; and DON production is induced during this interaction. In addition, *B. distachyon* reveals characteristics of a model plant that would support the identification of putative plant defense targets on functional as well as structural level: i) a short generation time with only simple growth requirements (Vogel & Bragg, 2009), ii) high-throughput genetic studies facilitated by the smallest genome size in the plant family of Poaceae with

little repetitive or methylated DNA (Draper *et al.*, 2001), iii) a publicly available genome sequence (International Brachypodium, 2010), iv) an easy genetic transformation system (Alves *et al.*, 2009, Christiansen *et al.*, 2005, Vogel & Hill, 2008), and v) a growing collection of T-DNA lines (Thole *et al.*, 2010).

Our study was aimed at evaluating the suitability of *B. distachyon* as a model for studying type II resistance to FHB in wheat caused by the fungal pathogen *F. graminearum*. On the one hand, we wanted to know whether similar type II resistance mechanisms are induced in *B. distachyon* like in wheat during interaction with well defined *F. graminearum* mutants. Type II resistance generally describes plant defense mechanisms that do not prevent initial infection but stop subsequent propagation of the pathogen, e.g. within the cereal spike (Schroeder & Christensen, 1963). The *F. graminearum* mutants that we chose for infection of *B. distachyon* revealed similar disease phenotypes on susceptible wheat even though phenotypes were caused by disruption of different virulence factors. The Δ*tri5* mutant is unable to produce the mycotoxin DON due to disruption of the trichodiene synthase gene *TRI5* (*TRICHODIENE SYNTHASE 5*) encoding for the first enzyme in the trichothecene pathway. On wheat, this mutant revealed initial infection of inoculated spikelets, but failed to penetrate the transition zone of the rachilla and rachis, the rachis node, for further colonization of the spike. Cell wall thickenings and appositions were detected at the rachis node during infection with this mutant, which were not formed during infection with the *F. graminearum* wild-type (Jansen *et al.*, 2005, Proctor *et al.*, 1995). A similar barrier formation was observed during wheat infection with the Δ*fgl1* mutant. The disrupted *FGL1* (*FUSARIUM GRAMINEARUM LIPASE1*) gene encodes a secreted lipase, which is required to break type II resistance in wheat (Voigt *et al.*, 2005) due to the release of polyunsaturated free fatty acids that can inhibit pathogen-

induced callose deposition in the phloem of infected spikelets (Blümke *et al.*, 2014). We included the Gpmk1 (Gibberella pathogenicity MAP kinase1) disruption mutant Δ*gpmk1* as an additional *F. graminearum* mutant (Jenczmionka *et al.*, 2003). The substantially reduced virulence of this mutant is largely based on a strong delay of *FGL1* induction (Bluhm *et al.*, 2007, Salomon *et al.*, 2012).

One of our main interests was to examine whether pathogen infection would induce changes of the non-cellulosic monosaccharide composition of the cell wall in the host model grass *B. distachyon*. This approach referred to our recent study in the model plant *Arabidopsis thaliana* where analysis of the non-cellulosic monosaccharide composition suggests that cell wall modifications might be involved in the determination of fungal resistance (Ellinger *et al.*, 2013).

Our infection with the *F. graminearum* mutant strains showed that *B. distachyon* induces similar type II defense mechanism like wheat, which confirmed the suitability of this model grass in *F. graminearum* interactions. The analysis of the host cell wall after *F. graminearum* infection revealed that the mycotoxin DON is involved in pathogen-induced modification. Similar changes of the host cell wall were also induced by DON application at relatively low concentrations without fungal infection. A low-dose DON pretreatment of *B. distachyon* spikelets prior *F. graminearum* infection supported type II resistance and reduced FHB disease symptoms. The analysis of cell wall composition and pathogen-related gene expression after DON application and subsequent *F. graminearum* infection indicated that DON-induced priming of the spikelet tissue contributed to the reduction of FHB disease symptoms of pretreated *B. distachyon* spikelets.

RESULTS

Infection progress of *F. graminearum* wild-type and mutants in *B. distachyon* spikelets

To investigate the potential of *B. distachyon* as a model host for studying type II resistance mechanisms to *F. graminearum*, we point-inoculated single florets of spikelets with conidia of *F. graminearum* wild-type and the defined, virulence-deficient mutants Δ*tri5*, Δ*fgl1*, and Δ*gpmk1*, which all constitutively expressed the green fluorescence protein GFP to visualize fungal growth *in planta*. The infection progress was monitored for 2 weeks until ripening started at the growth stage 85 referring to the BBCH (Biologische Bundesanstalt, Bundessortenamt and CHemische Industrie) scale (Hong *et al.*, 2011). Statistical analysis of the infection progress was achieved by calculation of the disease score at 5, 7, 11, and 14 d post-inoculation (dpi) where a score of ≥ 2 indicates a successful fungal colonization of additional florets other than the directly inoculated (Fig. 1).

As expected from inoculation of wheat spikes, the *F. graminearum* wild-type strain wt-GFP induced strongest disease symptoms on *B. distachyon* spikelets. The mycelium colonized the whole spikelet and spread through the rachilla from one floret to another (Fig. 2A). The disease score continuously increased during the monitored two weeks of infection, starting with 0.6 at 5 dpi and reaching a final score of 2.3 at 14 dpi (Fig. 2E). In wheat, *F. graminearum* requires DON production during infection to break type II resistance and to fully colonize the spike (Proctor *et al.*, 1995). The disruption of the trichodiene synthase TRI5 in the *F. graminearum* mutant Δ*tri5* prevents DON biosynthesis, which results in reduced virulence of the mutant. In contrast to *F. graminearum* wild-type, the Δ*tri5* mutant is not able to spread through

the rachis and to colonize the whole wheat spike (Jansen *et al.*, 2005). In *B. distachyon*, we observed a similar disease phenotype for the *TRI5* disruption mutant Δ*tri5*-GFP. This mutant failed to cross the rachilla and infection was restricted to the directly inoculated floret (Fig. 2B). A disease score of 1.2 at 14 dpi (Fig. 2E) reflected the reduced virulence compared to wild-type. Besides DON, the secreted lipase FGL1 is required for full virulence of *F. graminearum* on wheat (Voigt *et al.*, 2005). Similar to Δ*tri5*, the lipase disruption mutant Δ*fgl1* can only colonize directly inoculated wheat spikelets (Voigt *et al.*, 2005, Blümke *et al.*, 2014). In the initial phase of *B. distachyon* infection, Δ*flg1*-GFP exhibited a hyphal propagation within the directly inoculated floret, which was similar to the wt-GFP infection. However, the infection of the Δ*flg1*-GFP mutant was restricted to the directly inoculated floret (Fig. 2C). A disease score of 1.2 at 11 and 14 dpi confirmed this observation (Fig. 2E). The disruption of the MAP kinase Gpmk1 in the mutant Δ*gpmk1*-GFP (Salomon *et al.*, 2012) resulted in a strongly reduced virulence on *B. distachyon* that was similar to the phenotype reported from wheat (Jenczmionka & Schäfer, 2005, Urban *et al.*, 2003). In *B. distachyon*, we observed a slight hyphal growth of the Δ*gpmk1*-GFP mutant only at the point of direct inoculation within the floret (Fig. 2D). The relatively low disease score with a maximum of 0.2 (Fig. 2E) reflected the inability of this mutant to colonize the host.

Deoxynivalenol production of *F. graminearum* wild-type and mutants in *B. distachyon*

To analyze the production of DON by the different *F. graminearum* mutants during infection of *B. distachyon* spikelets, we determined the relative DON amount in the floral tissue. At 7 dpi, the infection with wt-GFP resulted in the highest DON

concentration (8.6 mg DON/g dry mycelium). We detected less DON in Δ*fg1l*-GFP infected tissue (5.8 mg/g); and the Δ*gpmk1*-GFP mutant produced only a small amount of DON on *B. distachyon* spikelets (0.9 mg/g) (Fig. 2F) at this time-point of infection. At 14 dpi, the relative DON amount of wt-GFP, Δ*fgl1*-GFP as well as Δ*gpmk1*-GFP infected tissue was comparable and reached a value of about 12 mg DON/g dry mycelium (Fig. 2F), which was similar to the relative DON amounts that were previously reported from *F. graminearum*-infected wheat spikes (Bormann *et al.*, 2014). As expected from determinations in wheat (Jansen *et al.*, 2005, Maier *et al.*, 2006), we did not detect DON in spikelet tissue infected with the Δ*tri5*-GFP mutant (Fig. 2F).

Host cell wall changes during *F. graminearum* infection and DON application

Because the plant cell wall represents the first line of defense against intruding pathogen; and alteration of the cell wall could be involved in pathogen resistance (Ellinger *et al.*, 2013), we determined the non-cellulosic monosaccharide composition of *B. distachyon* spikelet tissue after *F. graminearum* infection using high-performance anion-exchange chromatography with pulsed amperometric detection (HPAEC-PAD). The relative amounts of the main non-cellulosic cell wall components xylose (ca. 70 mol%), glucose (ca. 13 mol%), arabinose (ca. 12 mol%), and galactose (ca. 2 mol%) that we detected in water-inoculated control samples 7 dpi (Fig. 3A), were comparable to the amounts described in previous reports of *B. distachyon* and other grasses (Christensen *et al.*, 2010, Gomez *et al.*, 2008). Infection of *B. distachyon* with *F. graminearum* wt-GFP, Δ*fgl1*-GFP, and Δ*gpmk1*-GFP but not Δ*tri5*-GFP altered the spikelet's monosaccharide composition. At 7 dpi, the relative glucose content of wt-GFP- and Δ*fgl1*-GFP-infected spikelets was

slightly, and of Δ*gpmk1*-GFP-infected spikelets significantly increased, reaching a content of almost 18 mol% (Fig. 3A). Apart from glucose, we did not observed alterations for the other neutral monosaccharides (Fig. 3A). At 14 dpi, we observed a shift in the glucose/xylose ratio in the water-inoculated control tissue where the glucose content increased to almost 30 mol%, which correlated with a decrease in the xylose content to 58 mol%. The relative amounts of arabinose and galactose remained unchanged compared to 7 dpi, which also applied to the *F. graminearum*-infected samples for these monosaccharides (Fig. 3B). Whereas we did not detect differences in the cell wall composition between control and Δ*tri5*-GFP-infected samples, infection of spikelets with the *F. graminearum* strains wt-GFP, Δ*fgl1*-GFP, and Δ*gpmk1*-GFP resulted in a significant increase in the glucose amount compared to control tissue (Fig. 3B). Here, the relative glucose amount reached values of almost 40 mol%, which was about 30% higher than in control samples.

The analysis of the cell wall composition of spikelet tissue revealed that major changes in the glucose content compared to control tissue only occurred after inoculation with those *F. graminearum* strains that were able to produce the mycotoxin DON during *B. distachyon* infection (Fig. 2F). Therefore, we tested whether DON alone would be sufficient to induce cell wall changes in the host plant. We applied DON solutions at concentrations ranging from 1 ppb to 500 ppm to unchallenged *B. distachyon* florets. Seven days after DON application, we observed necrotic tissue especially at those spikelets that were treated with the highest DON concentration of 500 ppm (Fig. 4A). We occasionally found small necrotic lesions at spikelets treated with DON concentrations of 50 and 100 ppm whereas lower DON concentration (1 ppb to 1 ppm) did not induce necrotic lesions. However, application of relatively low-concentrated DON resulted in an increase in the non-cellulosic

glucose content of the treated spikelet tissue, which was most prominent for concentrations ranging from 1 to 100 ppb where the relative glucose content was almost twice as high as in control samples. This increase in glucose content correlated with a slightly decreased xylose content (Fig. 4B). We did not observe an alteration in the glucose content after application of DON concentration ranging from 50 to 500 ppm (Fig. 4B). The other two neutral monosaccharides arabinose and galactose were not affected in DON-treated tissue compared to control tissue (Fig. 4B).

DON-induced reduction of susceptibility to *F. graminearum* in *B. distachyon* spikelets

Our observations revealed that DON treatment induced cell wall changes in *B. distachyon* spikelet tissue, which revealed similarities to *F. graminearum*-induced cell wall changes during spikelet infection (Figs. 3 and 4B). Therefore, we tested whether DON-induced, putatively defense-related cell wall changes prior infection would support resistance of the *B. distachyon* spikelet to *F. graminearum* infection. We sprayed untreated *B. distachyon* spikelets with a DON solution at a concentration of 1 ppm to induce previously observed cell wall changes, which mainly affected the glucose content (Fig. 4B), and with water as control 7 d prior anthesis. Subsequently, we inoculated the pretreated spikelets with *F. graminearum* wt-GFP at anthesis and determined the disease phenotype 14 dpi. The water-pretreated spikelets revealed the same FHB disease phenotype that affected most parts of spikelet as we previously observed with untreated spikelets (Figs. 1A and 5A). In contrast to control spikelets, only the directly inoculated floret became necrotic in DON-pretreated spikelets after infection (Fig. 5A). These observations were statistically confirmed by the drop of the

disease score from 2.7 of water-pretreated spikelets to 1.6 of DON-pretreated spikelets at 14 dpi with *F. graminearum* wt-GFP (Fig. 5B).

To analyze the putative basis of the observed resistance in DON-pretreated spikelets, we compared non-cellulosic cell wall composition and expression of plant defense-related genes before and after *F. graminearum* infection in control and pretreated tissue. Similar to our previous results with a direct DON treatment at relatively low concentrations (Fig. 4B), also DON spraying of the spikelet induced cell wall changes. The relative glucose content in DON-pretreated spikelets was significantly higher than in water-sprayed control spikelets at the time-point of *F. graminearum* inoculation (time-point of anthesis, 7 d after spraying), reaching a value of 20 mol% compared to 14 mol% in control tissue (Fig. 5C). The impact of the DON pretreatment on cell wall alteration was strongly enhanced after *F. graminearum* infection. At 14 dpi, the relative glucose content increased from about 30 mol% in untreated spikelet tissue to 38 mol% in infected spikelets, which were only pretreated with water, whereas the glucose amount reached about 55 mol% in DON-pretreated and subsequently inoculated spikelets (Fig. 5C). Only in this pretreated and infected tissue, the relative xylose was reduced compared to control tissue. With a relative amount of about 45 mol%, the xylose content was lower than the glucose content in this tissue (Fig. 5C).

Similar to the observed cell wall changes after DON pretreatment, we observed both, a direct effect on gene expression prior infection and strong induction of gene expression after infection. The expression analysis comprised genes that showed highest homology to *F. graminearum*- and DON-responsive genes in barley (*Hordeum vulgare*) and wheat, which were the pathogenesis-related genes *BdPR1.1* and *BdPR2*, the putative UDP-glucosyltransferase gene *BdUGT*, the mitogen-

activated protein (MAP) kinase kinase kinase gene *BdMAPKKK* as well as *BdXET*, encoding a putative xyloglucosyl transferase with a possible involvement in the observed alterations of the cell wall composition after DON application and *F. graminearum* infection (Fig. 5C).

We detected a transcriptional upregulation after DON pretreatment and prior infection only for *BdXET* where the expression level was 3.5-times higher than in control tissue. Also 7 days post-inoculation, the expression of *BdXET* was higher in DON-pretreated tissue than in control tissue (Fig. 5D). Whereas we did not observe a pathogen-induced increase in *BdXET* expression in floret tissue that was only water-pretreated, a strong induction of *BdXET* expression occurred in DON-pretreated and *F. graminearum*-infected tissue where the expression level was about five-times higher than in infected, water-pretreated tissue (Fig. 5D). We also measured a strong induction of gene expression after infection for *BdPR1.1* and *BdPR2*. However, DON pretreatment did not affect gene expression prior infection, but strongly promoted transcriptional upregulation after infection (Fig. 5D). At 7 dpi, *BdPR1.1* expression was about four-times higher in infected floral tissue pretreated with water only than in unchallenged tissue, but 135-times higher in infected and DON-pretreated tissue (Fig. 5D). We had a similar result for *BdPR2* where expression was about seven-times higher in infected and water only-pretreated tissue, but 30-times higher in infected and DON-pretreated tissue than in control tissue (Fig. 5D). For *BdUGT*, we observed a transcriptional upregulation only after combined DON pretreatment and *F. graminearum* infection (Fig. 5D). In contrast, transcriptional upregulation of *BdMAPKKK* seemed to be independent of a DON pretreatment because the gene expression level was twice as high in infected tissue with and without DON pretreatment than in control tissue (Fig. 5D).

DISCUSSION

In our study, we confirmed previous results about the general suitability of *B. distachyon* as host plant for the agronomically important plant pathogenic fungus *F. graminearum*. Similar to the disease phenotype that Peraldi *et al.* (2011) described for *B. distachyon* after infection with the *F. graminearum* isolate UK1, we observed a strong colonization of the *B. distachyon* spikelet by the GFP-tagged *F. graminearum* isolate 8/1 (Fig. 2A) that we used in our experiments. In both studies, the disease phenotype at 14 dpi with *F. graminearum* resembled FHB disease symptoms that were reported from wheat head infection with this fungal pathogen (Walter *et al.*, 2010, Blümke *et al.*, 2014). Besides the macroscopically observed similarity of the FHB disease phenotype in wheat and *B. distachyon*, the induction and production of the mycotoxin DON by *F. graminearum* in *B. distachyon* spikelets (Fig. 2F) was comparable to the DON concentration determined in infected wheat heads (Nguyen *et al.*, 2011, Peraldi *et al.*, 2011, Bormann *et al.*, 2014). In addition to *F. graminearum* wild-type, we were able to show that also defined, virulence-deficient *F. graminearum* mutant strains induced a similar disease phenotype during *B. distachyon* infection as previously reported from infected wheat heads. The infection of the DON-deficient disruption mutant Δ*tri5*-GFP as well as the infection of the lipase disruption mutant Δ*fgl1*-GFP was restricted to the directly inoculated floret (Fig. 2B, C, and E), which resembled the importance of these *F. graminearum* virulence factors during *B. distachyon* infection as previously reported from wheat infection (Jansen *et al.*, 2005, Proctor *et al.*, 1995, Voigt *et al.*, 2005, Blümke *et al.*, 2014). The strongly reduced disease phenotype of the MAP-kinase disruption mutant Δ*gpmk1* reported from wheat (Jenczmionka *et al.*, 2003) was also confirmed on *B.*

distachyon spikelets (Fig. 2D, E). This suggests the presence of comparable type II defense mechanisms (Schroeder & Christensen, 1963) in these Triticeae species and supports the applicability of the model pathosystem *B. distachyon – F. graminearum* for studying and modifying essential plant defense response to improve fungal resistance.

Regarding plant defense, we focused on cell wall changes of *B. distachyon* spikelets that were infected with *F. graminearum* wild-type and the virulence-deficient mutants Δ*tri5*-GFP, Δ*fgl1*-GFP, and Δ*gpmk1*-GFP. Because the plant cell wall represents a main barrier against intruding pathogens that can be actively remodeled after infection (Sanchez-Rodriguez *et al.*, 2009, Underwood, 2012), we anticipated a correlation between the strength of the infection and the alteration of the cell wall composition. However, we found a correlation between *F. graminearum* strains with intact DON production and plant cell wall changes but not between the strength of infection and cell wall changes (Figs. 2F and 3B). Therefore, we wanted to know whether the mycotoxin DON alone would be sufficient to induce those cell wall changes that we observed after infection with DON-producing *F. graminearum* strains. In *B. distachyon* spikelets that were point-inoculated with DON solutions at relatively low concentrations ranging from 1 ppb to 100 ppb, we determined an increase in glucose content in the non-cellulosic monosaccharide faction 7 d after DON application (Fig. 4B). The applied higher DON concentrations of 50 ppm to 500 ppm did not induce cell wall changes but led to necroses of the inoculated florets (Fig. 4A), which we did not find after application of low-concentrated DON. The fact that DON induces disease symptoms including necrosis and chlorosis (Cutler, 1988, Peraldi *et al.*, 2011), has been associated with the protein synthesis-inhibiting properties of DON through binding to the 60S ribosomal subunit of eukaryotes and induction of

ribosomal RNA cleavage, which can result in hypersensitive responses and cell death (Kimura *et al.*, 1998, Rocha *et al.*, 2005, Zhou *et al.*, 2005, He *et al.*, 2012).

Because the polysaccharide composition of the plant cell wall has been proposed to play a role in host-pathogen interactions (Vorwerk *et al.*, 2004), which is also indicated by our recent study in *A. thaliana* (Ellinger *et al.*, 2013), we assumed that the increase in glucose content of the non-cellulosic monosaccharide fraction of the cell wall could be an indicator of a pathogen- and DON-induced plant defense reaction. Therefore, we tested whether a pretreatment of floral tissue with low-concentrated DON would increase resistance to subsequent *F. graminearum* infection. Interestingly, the DON pretreatment of *B. distachyon* spikelets resulted in an increased resistance to *F. graminearum* wild-type (Fig. 4A, B). Because the disease phenotype resembled the phenotype observed after infection with the virulence-deficient mutants Δ*tri5*-GFP and Δ*fgl1*-GFP (Fig. 2B, C), we concluded that application of DON at a relatively low concentration might activate defense mechanisms that induce a type II resistance in the host floral tissue. Moreover, the analysis of the cell wall composition and the expression of genes that were previously reported to be associated to a pathogen- and DON-dependent stress response, suggests that a low-dose DON pretreatment could have a dual effect on triggering plant defense responses. On the one hand, we identified cell wall changes that were induced by low-dose DON application without subsequent pathogen infection, namely the increased non-cellulosic glucose content. Because the expression of the putative xyloglucan xyloglucosyl transferase encoding gene *BdXET* correlated with the observed changes of the plant cell wall (Fig. 5C, D), it is likely that these DON-induced cell wall alterations would be the result of DON-induced transcriptional changes of genes encoding cell wall-modifying enzymes. The extent to which the

observed cell wall change, namely the DON-induced increase in glucose in the non-cellulosic fraction, is a direct defense response of the plant cannot be conclusively answered. Because reference data for pathogen- and mycotoxin-induced cell wall modifications and their consequence on host-pathogen interaction for grasses are not available, our data could be considered as a starting point for additional cell wall analyses. Interestingly, the observed increased resistance of tobacco (*Nicotiana tabacum*) to the fungal pathogen *Botrytis cinerea* due to overexpression of polygalacturonase-inhibiting protein from grapevine (*Vitis vinifera*) was associated with a reorganization of the cellulose-xyloglucan network in advance of infection (Nguema-Ona *et al.*, 2013). Further cell wall studies in *B. distachyon* might reveal whether the DON- and pathogen-induced increase in the glucose content would also be a consequence of the cellulose-xyloglucan network modification.

On the other hand, we observed a hyperactivation of pathogenesis-related gene expression in DON-pretreated spikelet tissue after *F. graminearum* infection. Unlike *BdXET*, the expression of the two analyzed pathogenesis-related genes *BdPR1.1* and *BdPR2* in DON-pretreated tissue was not different from control tissue without infection. As expected from pathogenesis-related genes, the expression of *BdPR1.1* and *BdPR2* was induced after *F. graminearum* infection of untreated *B. distachyon* spikelets; however, gene expression was 30-times higher for *BdPR1.1* and four-times higher for *BdPR2* in DON-pretreated tissue after infection (Fig. 5D). Hence, resistance to FHB could be based on the hyperactivation of pathogenesis-related genes, which would support plant defense reactions and type II resistance.

The observed hyperactivation of plant defense responses after DON-pretreatment shows clear similarities to defense priming of plants, a process of enhanced activation of defense responses following the recognition of pathogen-derived molecular pattern,

effectors, or compound treatment (Conrath, 2011). In primed plants, the enhanced activation of plant defense is often linked with local and systemic resistance leading to higher stress and pathogen tolerance (Conrath *et al.*, 2006, Conrath *et al.*, 2002, Jung *et al.*, 2009). In this concept of plant defense priming, DON, if applied at a relatively low concentration, would function as a cellular signal amplifier (Conrath, 2011) resulting in enhanced defense. In contrast to low-dose DON application and the associated priming effect in *B. distachyon*, Peraldi *et al*. (2011) showed that high-concentrated DON not only induced lesions and necroses but also strongly supported the *F. graminearum* infection of *B. distachyon*.

A dose-dependent effect of the mycotoxin DON on immunity was also shown in animal systems where DON targets monocytes, macrophages, and lymphocytes of the immune system. Mice fed with sublethal doses of 0.5 and 1.0 mg DON/kg body weight per day in their basal diet showed a significant reduction in the serum levels of alpha-1- and alpha-2-globulins and a reduced time-to-death interval when challenged with the infectious bacterium *Listeria monocytogenes* whereas a DON dose of 0.25 mg/kg did not influenced these parameters (Tryphonas *et al.*, 1986). One reason for the DON-induced symptoms in mice is a modulation of genes associated with immunity, inflammation, and chemotaxis (Kinser *et al.*, 2004), which was recently confirmed in chicken fed with basal diet contaminated with DON (Ghareeb *et al.*, 2013). Further *in vitro* analysis of the dose-dependent effect of DON on immunity revealed that an immune stimulation followed a transcriptional upregulation of cytokines, chemokines, and inflammatory genes at low DON concentrations, whereas high DON concentrations induced a ribotoxic stress response, which promoted leukocyte apoptosis. The intracellular DON signaling involved different kinases, including MAP kinases and RNA-activated protein kinases, that were activated after

the binding of DON to ribosomes (He *et al.*, 2012, Pestka, 2008). Interestingly, dormant MAP kinases accumulated during priming in *A. thaliana* (Beckers *et al.*, 2009) and supported the assumption that kinases play a key role in the molecular mechanisms and signaling pathways of defense priming.

Therefore, plant kinases and especially MAP kinases would constitute a promising target in gene expression and protein studies after DON application to elucidate the DON signaling pathway in plants leading to plant defense priming because MAP kinases would represent a link between the known mode of action of DON in eukaroytes, which is the binding to ribosomes, and the molecular basis of priming in plants.

EXPERIMENTAL PROCEDURES

Plant material and growth conditions

B. distachyon (L.) Beauv. inbred line Bd21 (Vogel *et al.*, 2006) was cultivated in 2 parts of soil (Einheitserdewerk Uetersen, Germany, ED 73 + 10% sand) and one part of sand at 22°C and a 20 h photoperiod in a growth chamber. Approximately 6 weeks after sowing the plants reached anthesis and were inoculated. After inoculation plants were transferred in growth cabinet and grown for 14 d at 22°C, at a photoperiod of 16 h and 50 - 60% humidity.

Fungal strains and culture conditions

All fungal mutants used in this study originated from the transformation of the *F. graminearum* isolate Fg 8/1 (Miedaner *et al.*, 2000). The trichodiene synthase disruption mutant Δ*tri5*-GFP with constitutive GFP expression derived from the study of Jansen *et al.* (2005); the Gpmk1 MAP-kinase disruption mutant Δ*gpmk1-GFP* with constitutive GFP expression derived from the study of Salomon *et al*. (2012); and the GFP-expressing wild-type strain wt-GFP as well as the GFP-expressing lipase-deficient disruption mutant *Δfgl1*-GFP derived from our recent study (Blümke *et al*. 2014). Media, induction of conidiation, and culture conditions were applied according to Jenzmionka *et al*. (2003). *F. graminearum* conidia were stored in aqueous suspensions at -70°C.

Plant inoculation

All plants were inoculated in the late afternoon. For infection studies with *F. graminearum*, the 3. or 4. floret of a *B. distachyon* spikelet was point-inoculated with 1 µL water, containing 40 conidia or with sterile water only as negative control at growth stages 61-65 (mid-anthesis) following the BBCH (Biologische Bundesanstalt, Bundessortenamt and CHemische Industrie) scale (Hong *et al.*, 2011). The conidia suspension was placed between lemma and palea. The floret was gently closed and the plant was covered with a plastic bag for two days to increase humidity and to promote fungal infection. Samples for cell wall analysis were taken 7 and 14 dpi. Repeat inoculation experiments were performed with the same -70°C conidia stock suspensions.

Point-inoculation of florets with 1 µl of DON solutions at different concentrations (1 ppb, 10 ppb, 100 ppb, 1 ppm, 50 ppm, 100 ppm, 500 ppm) and water only as control followed the above description for inoculation with conidia, except that plants were not covered with plastic bags after inoculation. Samples for cell wall analysis were taken 7 dpi.

Spray-inoculation of *B. distachyon* spikelets with a DON solution (concentration: 1 ppm) was performed 7 d before mid-anthesis (growth stage 55-53 (Hong *et al.*, 2011)). Spraying with water served as control. Samples for cell wall analysis were taken 7 d after spraying at the time-point of *F. graminearum* inoculation (0 dpi) and 14 dpi.

A single spikelet of at least 3 individual plants grown in separate pots was inoculated with fungal strains or treated with DON as described above. Inoculation experiments were repeated three-times in a weekly interval.

Disease scoring

At 14 dpi with *F. graminearum* when ripening started and no further infection progress was detectable, the infection was monitored using a numerical scoring system (Fig. 1). The infection was rated with 0.1 for a slight infection of a floret when only small brownish dots were visible on the caryopsis or the rachilla. A floret was rated 0.5 when the infection resulted in at least two necrotic spots and a maximum of 50% necrotic tissue. In the case of over 50% necrotic tissue, the floret was rated 1.0. For each spikelet, the single florets were examined and the score was calculated.

Microscopy

To visualize the spread and propagation of the *F. graminearum* strains within the infected floret and spikelet, a Nikon AZ100 fluorescence microscope was used in bright field microscopy and fluorescence microscopy with the filter B-2A (Nikon, Japan) with an excitation at 450-490 nm (epi-fluorescence illuminator C-HGFI, Nikon) to visualize GFP fluorescence emitted from tagged fungal strains.

DON quantification

To determine the concentration of the mycotoxin DON, inoculated *B. distachyon* florets were harvested 7 and 14 dpi with *F. graminearum*. At least 3 spikelets from individually inoculated plants of 4 biologically independent experiments were pooled (pool 1: spikelets from experiment 1, pool 2: spikelets from experiment 2, pool 3: spikelets from experiment 3 and 4; compare description in section “Plant inoculation”) ground under liquid nitrogen, and freeze dried. .

DON was extracted from 50 mg dried sample following the manufactor's instruction of the Ridascreen DON enzymatic immunoassay (R-Biopharm, Germany). The determined amount of DON was normalized to the amount of fungal mycelium in the respective plant tissue. Quantification of fungal mycelium was performed in real-time PCR analysis using DNA from dried fungal mycelium as a standard as previously described by Voigt *et al*. (2007).

Cell wall analysis

The determination of the non-cellulosic monosaccharide composition of the cell wall from *B. distachyon* spikelet tissue followed the description in Ellinger *et al*. (2013). Extracted monosaccharides were quantified by high-performance anion-exchange chromatography with pulsed amperometric detection (HPAEC-PAD) on an ICS-5000 system equipped with an electrochemical detector and a CarboPac PA 20 column (Dionex, USA). Fucose, arabinose, rhamnose, galactose, mannose, xylose, glucose, glucuronic acid, and galacturonic acid (all from Sigma-Aldrich, Germany) were used as standards. Generation of 3 pools of spikelets for cell wall analysis followed the description in section "DON quantification".

Quantitative real-time PCR

To study gene expression in *B. distachyon* before and after *F. graminearum* infection, samples were collected from spikelets that were sprayed with DON or water only as control at the time-point of *F. graminearum* inoculation (0 dpi) and 7 dpi. Samples without fungal inoculation served as control. For RNA isolation, complete spikelets were used. Generation of 3 pools of spikelets for quantitative real-time PCR (qPCR) followed the description in section "DON quantification". Subsequent procedures for

RNA isolation and cDNA generation were performed according to Voigt *et al*. (2006). qPCR was performed on a LightCyler 480 (Roche Diagnostics, Germany) using the LightCycler 480 SYBR Green I Master mix (Roche). In qPCR reactions, cDNA samples were normalized against constitutive *Actin* gene (Gramene database (Monaco *et al.*, 2014): Bradi4g41850; primer: fwd 5'- GCTGGGCGTGACCTAACTGAC, rev 5'-ATGAAAGATGGCTGGAAAAGGACT) expression.

Genes used for expression analysis were identified based on their sequence homology to known *F. graminearum*- and DON-induced genes in wheat and barley. The pathogenesis-related genes *BdPR1.1* (Bradi1g57540; fwd 5'-AAGAACGCCGTGGACATGTG, rev 5'-ACCCGGAGGATCATAACTAC) and *BdPR2* (Bradi2g60490; fwd 5'-AGCCATCCAGCTCAACTAC, rev 5'-CCTTGCCAACATGGTCAATC) showed highest homology to respective wheat genes with a transcriptional induction after DON treatment (Desmond *et al.*, 2008), the putative UDP-glycosyltransferase encoding gene *BdUGT* (Bradi2g05050; fwd 5'-CGCGGCTTCCGTGGTGTA, rev 5'-GTTGCCGTCGCCCACGTC) and the putative MAP kinase kinase kinase gene *BdMAPKKK* (Bradi2g17840; fwd 5'-CCATGCCGACCTTGATAGAG, rev 5'-CCTGAAACTTTGGGCGAGAG) showed highest homology to respective *F. graminearum*- and DON-induced barley genes (Boddu *et al.*, 2007), and *BdXET* (Bradi1g33827; fwd 5'-AGCACAGGAACAGGGAGAC, rev 5'- GTCCAGCTCCTGGTACATC) with highest homology to the cell wall modifying xyloglucan xyloglucosyl transferase gene *XET6* from barley (Hrmova *et al.*, 2009).

Statistical analysis

Statistical analysis was performed using SPSS Statistics (release 20.0.0, IBM, USA). Parametric data from the disease score, DON content and monosaccharide composition were analyzed by means using one-way Analysis of Variance (ANOVA), followed by a Dunnett post-hoc test to identify significant samples. If variance was not homogeneous, data were compared via Welch (*t* test) tests. $p < 0.05$ was considered significant. All statistical values represent the mean of the respective dataset and error bars the standard error of the mean (± SEM).

ACKNOWLEDGEMENTS

We would like to thank John Vogel for providing the seeds of the *B. distachyon* inbred line Bd21, and Wilhelm Schäfer for providing the *F. graminearum* strain Δ*tri5*-GFP.

REFERENCES

Alves, S. C., Worland, B., Thole, V., Snape, J. W., Bevan, M. W. and Vain, P. (2009) A protocol for Agrobacterium-mediated transformation of *Brachypodium distachyon* community standard line Bd21. *Nat. Protocols,* **4,** 638-649.

Beckers, G. J., Jaskiewicz, M., Liu, Y., Underwood, W. R., He, S. Y., Zhang, S. and Conrath, U. (2009) Mitogen-activated protein kinases 3 and 6 are required for full priming of stress responses in *Arabidopsis thaliana*. *Plant Cell,* **21,** 944-953.

Blümke, A., Falter, C., Herrfurth, C., Sode, B., Bode, R., Schäfer, W., Feussner, I. and Voigt, C. A. (2014) Secreted fungal effector lipase releases free fatty acids to inhibit innate immunity-related callose formation during wheat head infection. *Plant Physiol.,* **165,** 346-358.

Bluhm, B. H., Zhao, X., Flaherty, J. E., Xu, J. R. and Dunkle, L. D. (2007) RAS2 regulates growth and pathogenesis in *Fusarium graminearum*. *Mol. Plant-Microbe Interact.,* **20,** 627-636.

Boddu, J., Cho, S. and Muehlbauer, G. J. (2007) Transcriptome analysis of trichothecene-induced gene expression in barley. *Mol. Plant-Microbe Interact.,* **20,** 1364-1375.

Bormann, J., Boenisch, M. J., Bruckner, E., Firat, D. and Schäfer, W. (2014) The adenylyl cyclase plays a regulatory role in the morphogenetic switch from vegetative to pathogenic lifestyle of *Fusarium graminearum* on wheat. *PLoS One,* **9,** e91135.

Buerstmayr, H., Ban, T. and Anderson, J. A. (2009) QTL mapping and marker-assisted selection for Fusarium head blight resistance in wheat: a review. *Plant Breeding,* **128,** 1-26.

Catalán, P., Shi, Y., Armstrong, L., Draper, J. and Stace, C. A. (1995) Molecular phylogeny of the grass genus *Brachypodium* P. Beauv. based on RFLP and RAPD analysis. *Bot. J. Linn. Soc.,* **117,** 263-280.

Chakraborty, S. and Newton, A. C. (2011) Climate change, plant diseases and food security: an overview. *Plant Pathol.,* **60,** 2-14.

Christensen, U., Alonso-Simon, A., Scheller, H. V., Willats, W. G. T. and Harholt, J. (2010) Characterization of the primary cell walls of seedlings of *Brachypodium distachyon* - A potential model plant for temperate grasses. *Phytochem.,* **71,** 62-69.

Christiansen, P., Andersen, C. H., Didion, T., Folling, M. and Nielsen, K. K. (2005) A rapid and efficient transformation protocol for the grass *Brachypodium distachyon*. *Plant Cell Rep.,* **23,** 751-758.

Conrath, U. (2011) Molecular aspects of defence priming. *Trends Plant Sci.,* **16,** 524-531.

Conrath, U., Beckers, G. J., Flors, V., Garcia-Agustin, P., Jakab, G., Mauch, F., Newman, M. A., Pieterse, C. M., Poinssot, B., Pozo, M. J., Pugin, A., Schaffrath, U., Ton, J., Wendehenne, D., Zimmerli, L. and Mauch-Mani, B. (2006) Priming: getting ready for battle. *Mol. Plant-Microbe Interact.,* **19,** 1062-1071.

Conrath, U., Pieterse, C. M. and Mauch-Mani, B. (2002) Priming in plant-pathogen interactions. *Trends Plant Sci.,* **7,** 210-216.

Cowger, C. and Sutton, A. L. (2005) The southeastern U.S. Fusarium head blight epidemic of 2003. In: *Plant Health Prog.*

Cutler, H. G. (1988) Trichothecenes and Their Role in the Expression of Plant Disease. In: *Biotechnology for Crop Protection.* American Chemical Society, pp. 50-72.

del Blanco, I. A., Frohberg, R. C., Stack, R. W., Berzonsky, W. A. and Kianian, S. F. (2003) Detection of QTL linked to Fusarium head blight resistance in Sumai 3-derived North Dakota bread wheat lines. *Theor. Appl. Genet.,* **106,** 1027-1031.

Desmond, O. J., Manners, J. M., Stephens, A. E., Maclean, D. J., Schenk, P. M., Gardiner, D. M., Munn, A. L. and Kazan, K. (2008) The *Fusarium* mycotoxin deoxynivalenol elicits hydrogen peroxide production, programmed cell death and defence responses in wheat. *Mol. Plant. Pathol.,* **9,** 435-445.

Draper, J., Mur, L. A., Jenkins, G., Ghosh-Biswas, G. C., Bablak, P., Hasterok, R. and Routledge, A. P. (2001) *Brachypodium distachyon*. A new model system for functional genomics in grasses. *Plant Physiol.,* **127,** 1539-1555.

Duveiller, E., Singh, R. P. and Nicol, J. M. (2007) The challenges of maintaining wheat productivity: pests, diseases, and potential epidemics. *Euphytica,* **157,** 417-430.

Ellinger, D., Naumann, M., Falter, C., Zwikowics, C., Jamrow, T., Manisseri, C., Somerville, S. C. and Voigt, C. A. (2013) Elevated early callose deposition results in complete penetration resistance to powdery mildew in Arabidopsis. *Plant Physiol.,* **161,** 1433-1444.

Ghareeb, K., Awad, W. A., Soodoi, C., Sasgary, S., Strasser, A. and Bohm, J. (2013) Effects of feed contaminant deoxynivalenol on plasma cytokines and mRNA expression of immune genes in the intestine of broiler chickens. *PLoS One,* **8,** e71492.

Gomez, L. D., Bristow, J. K., Statham, E. R. and McQueen-Mason, S. J. (2008) Analysis of saccharification in *Brachypodium distachyon* stems under mild conditions of hydrolysis. *Biotechnol. Biofuels,* **1,** 15.

He, K., Zhou, H. R. and Pestka, J. J. (2012) Targets and intracellular signaling mechanisms for deoxynivalenol-induced ribosomal RNA cleavage. *Toxicol. Sci.,* **127,** 382-390.

Hong, S. Y., Park, J. H., Cho, S. H., Yang, M. S. and Park, C. M. (2011) Phenological growth stages of *Brachypodium distachyon*: codification and description. *Weed Res.,* **51,** 612-620.

Hrmova, M., Farkas, V., Harvey, A. J., Lahnstein, J., Wischmann, B., Kaewthai, N., Ezcurra, I., Teeri, T. T. and Fincher, G. B. (2009) Substrate specificity and catalytic mechanism of a xyloglucan xyloglucosyl transferase HvXET6 from barley (*Hordeum vulgare* L.). *FEBS J.,* **276,** 437-456.

International Brachypodium, I. (2010) Genome sequencing and analysis of the model grass *Brachypodium distachyon*. *Nature,* **463,** 763-768.

Jansen, C., von Wettstein, D., Schafer, W., Kogel, K. H., Felk, A. and Maier, F. J. (2005) Infection patterns in barley and wheat spikes inoculated with wild-type and trichodiene synthase gene disrupted *Fusarium graminearum*. *Proc. Natl. Acad. Sci. U.S.A.,* **102,** 16892-16897.

Jenczmionka, N. J., Maier, F. J., Lösch, A. P. and Schäfer, W. (2003) Mating, conidiation and pathogenicity of *Fusarium graminearum*, the main causal agent of the head-blight disease of wheat, are regulated by the MAP kinase gpmk1. *Curr. Genet.,* **43,** 87-95.

Jenczmionka, N. J. and Schäfer, W. (2005) The Gpmk1 MAP kinase of *Fusarium graminearum* regulates the induction of specific secreted enzymes. *Curr. Genet.,* **47,** 29-36.

Jung, H. W., Tschaplinski, T. J., Wang, L., Glazebrook, J. and Greenberg, J. T. (2009) Priming in systemic plant immunity. *Science,* **324,** 89-91.

Kimura, M., Kaneko, I., Komiyama, M., Takatsuki, A., Koshino, H., Yoneyama, K. and Yamaguchi, I. (1998) Trichothecene 3-O-acetyltransferase protects both the producing organism and transformed yeast from related mycotoxins. *J. Biol. Chem.,* **273,** 1654-1661.

Kinser, S., Jia, Q., Li, M., Laughter, A., Cornwell, P., Corton, J. C. and Pestka, J. (2004) Gene expression profiling in spleens of deoxynivalenol-exposed mice: immediate early genes as primary targets. *J. Toxicol. Environ. Health A,* **67,** 1423-1441.

Madgwick, J. W., West, J. S., White, R. P., Semenov, M. A., Townsend, J. A., Turner, J. A. and Fitt, B. D. L. (2011) Impacts of climate change on wheat anthesis and fusarium ear blight in the UK. *Eur. J. Plant Pathol.,* **130,** 117-131.

Maier, F. J., Miedaner, T., Hadeler, B., Felk, A., Salomon, S., Lemmens, M., Kassner, H. and Schäfer, W. (2006) Involvement of trichothecenes in fusarioses of wheat, barley and maize evaluated by gene disruption of the trichodiene synthase (Tri5) gene in three field isolates of different chemotype and virulence. *Mol. Plant Pathol.,* **7,** 449-461.

McMullen, M., Jones, R. and Gallenberg, D. (1997) Scab of wheat and barley: A Re-emerging disease of devastating impact. *Plant Dis.,* **81,** 1340-1348.

Miedaner, T., Reinbrecht, C. and Schilling, A. G. (2000) Association among aggressiveness, fungal colonization, and mycotoxin production of 26 isolates of *Fusarium graminearum* in winter rye head blight. *J. Plant Dis. Protect. ,* **107,** 124-134.

Monaco, M. K., Stein, J., Naithani, S., Wei, S., Dharmawardhana, P., Kumari, S., Amarasinghe, V., Youens-Clark, K., Thomason, J., Preece, J., Pasternak, S., Olson, A., Jiao, Y., Lu, Z., Bolser, D., Kerhornou, A., Staines, D., Walts, B., Wu, G., D'Eustachio, P., Haw, R., Croft, D., Kersey, P. J., Stein, L., Jaiswal, P. and Ware, D. (2014) Gramene 2013: comparative plant genomics resources. *Nucleic Acids Res.,* **42,** D1193-1199.

Nguema-Ona, E., Moore, J. P., Fagerstrom, A. D., Fangel, J. U., Willats, W. G., Hugo, A. and Vivier, M. A. (2013) Overexpression of the grapevine PGIP1 in tobacco results in compositional changes in the leaf arabinoxyloglucan network in the absence of fungal infection. *BMC Plant Biol,* **13,** 46.

Nguyen, L. N., Bormann, J., Le, G. T., Stärkel, C., Olsson, S., Nosanchuk, J. D., Giese, H. and Schäfer, W. (2011) Autophagy-related lipase FgATG15 of *Fusarium graminearum* is important for lipid turnover and plant infection. *Fungal Genet. Biol.,* **48,** 217-224.

Peraica, M., Radic, B., Lucic, A. and Pavlovic, M. (1999) Toxic effects of mycotoxins in humans. *Bulletin of the World Health Organization,* **77,** 754-766.

Peraldi, A., Beccari, G., Steed, A. and Nicholson, P. (2011) *Brachypodium distachyon*: a new pathosystem to study Fusarium head blight and other Fusarium diseases of wheat. *BMC Plant Biol.,* **11,** 100.

Pestka, J. J. (2008) Mechanisms of deoxynivalenol-induced gene expression and apoptosis. *Food Addit. Contam. Part A Chem. Anal. Control Expo. Risk Assess.,* **25,** 1128-1140.

Proctor, R. H., Hohn, T. M. and McCormick, S. P. (1995) Reduced virulence of *Gibberella zeae* caused by disruption of a trichthecine toxin biosynthetic gene. *Mol. Plant-Microbe Interact.,* **8,** 1995-1908.

Rocha, O., Ansari, K. and Doohan, F. M. (2005) Effects of trichothecene mycotoxins on eukaryotic cells: A review. *Food Addit. Contam. Part A Chem. Anal. Control Expo. Risk Assess.,* **22,** 369-378.

Salomon, S., Gácser, A., Frerichmann, S., Kröger, C., Schäfer, W. and Voigt, C. (2012) The secreted lipase FGL1 is sufficient to restore the initial infection step to the apathogenic *Fusarium graminearum* MAP kinase disruption mutant *Δgpmk1*. *Eur. J. Plant Pathol.,* **134,** 23-37.

Sanchez-Rodriguez, C., Estevez, J. M., Llorente, F., Hernandez-Blanco, C., Jorda, L., Pagan, I., Berrocal, M., Marco, Y., Somerville, S. and Molina, A. (2009) The ERECTA receptor-like kinase regulates cell wall-mediated resistance to pathogens in *Arabidopsis thaliana*. *Mol. Plant-Microbe Interact.,* **22,** 953-963.

Schroeder, H. W. and Christensen, J. J. (1963) Factors affecting resistance of wheat to scab caused by *Gibberella zeae*. *Phytopathol.,* **53,** 831-838.

Thole, V., Worland, B., Wright, J., Bevan, M. W. and Vain, P. (2010) Distribution and characterization of more than 1000 T-DNA tags in the genome of *Brachypodium distachyon* community standard line Bd21. *Plant Biotechnol. J.,* **8,** 734-747.

Tryphonas, H., Iverson, F., So, Y., Nera, E. A., McGuire, P. F., O'Grady, L., Clayson, D. B. and Scott, P. M. (1986) Effects of deoxynivalenol (vomitoxin) on the humoral and cellular immunity of mice. *Toxicol. Lett.,* **30,** 137-150.

Underwood, W. (2012) The plant cell wall: a dynamic barrier against pathogen invasion. *Front. Plant Sci.,* **3,** 85.

Urban, M., Mott, E., Farley, T. and Hammond-Kosack, K. (2003) The *Fusarium graminearum* MAP1 gene is essential for pathogenicity and development of perithecia. *Mol. Plant. Pathol.,* **4,** 347-359.

Vogel, J. and Bragg, J. (2009) *Brachypodium distachyon*, a New Model for the Triticeae In: *Genetics and Genomics of the Triticeae.* Springer New York, pp. 427-449.

Vogel, J. and Hill, T. (2008) High-efficiency Agrobacterium-mediated transformation of *Brachypodium distachyon* inbred line Bd21-3. *Plant Cell Rep.,* **27,** 471-478.

Vogel, J. P., Gu, Y. Q., Twigg, P., Lazo, G. R., Laudencia-Chingcuanco, D., Hayden, D. M., Donze, T. J., Vivian, L. A., Stamova, B. and Coleman-Derr, D. (2006) EST sequencing and phylogenetic analysis of the model grass *Brachypodium distachyon*. *Theor. Appl. Genet.,* **113,** 186-195.

Voigt, C. A., Schäfer, W. and Salomon, S. (2005) A secreted lipase of *Fusarium graminearum* is a virulence factor required for infection of cereals. *Plant J.,* **42,** 364-375.

Voigt, C. A., Schäfer, W. and Salomon, S. (2006) A comprehensive view on organ-specific callose synthesis in wheat (*Triticum aestivum* L.): glucan synthase-like gene expression, callose synthase activity, callose quantification and deposition. *Plant Physiol. Biochem.,* **44,** 242-247.

Voigt, C. A., von Scheidt, B., Gácser, A., Kassner, H., Lieberei, R., Schäfer, W. and Salomon, S. (2007) Enhanced mycotoxin production of a virulence-reduced *Fusarium graminearum* mutant correlates to toxin-related gene expression. *Eur. J. Plant Pathol.,* **117,** 1-12.

Vorwerk, S., Somerville, S. and Somerville, C. (2004) The role of plant cell wall polysaccharide composition in disease resistance. *Trends Plant Sci.,* **9,** 203-209.

Walter, S., Nicholson, P. and Doohan, F. M. (2010) Action and reaction of host and pathogen during Fusarium head blight disease. *New Phytol.,* **185,** 54-66.

Zhou, H. R., Islam, Z. and Pestka, J. J. (2005) Induction of competing apoptotic and survival signaling pathways in the macrophage by the ribotoxic trichothecene deoxynivalenol. *Toxicol. Sci.,* **87,** 113-122.

FIGURE LEGENDS

Figure 1. Numeric scoring system for rating the disease severity of *F. graminearum*-infected *B. distachyon* spikelets.

(A) Uninfected floret, disease score: 0.0.

(B) Weak infection of a floret, only one small, restricted necrosis (N) visible on the caryopsis or the rachilla, disease score: 0.1.

(C) More than one necrotic lesion and/or lesion(s) covering a maximum of 50 % of the infected floret, disease score: 0.5.

(D) Extended necrosis covering more than half of the floret, highest disease score of 1.0. For each spikelet, single florets were rated 14 d post-inoculation with *F. graminearum* strains and the score was calculated as indicated in the formula. L, lemma. Scale bar = 2 mm.

Figure 2. Disease phenotype and DON accumulation in *B. distachyon* spikelets after *F. graminearum* infection.

(A-D) Micrographs of longitudinal sectioned spikelets 14 d post-inoculation (dpi) with the GFP-tagged *F. graminearum* strains: (A) wild-type wt-GFP, (B) DON-deficient disruption mutant Δ*tri5*-GFP, (C) lipase-deficient disruption mutant Δ*flg1*-GFP, and (D) MAP kinase-deficient disruption mutant Δ*gpmk1*-GFP. Left panels: images of spikelet sections with bright field illumination to visualize necrotic tissue; mid-panels: images of same sections as in left panels, but with epi-fluorescent illumination to visualize GFP-emitting fungal hyphae; and right panels: magnification of the rachilla of inoculated florets with epi-fluorescent illumination. Scale bars for left and mid-panels = 2 mm, for right panels = 0.2 mm.

(E) Disease score of infected spikelets 5, 7, 11, and 14 dpi with GFP-tagged *F. graminearum* strains as indicated. *$p < 0.05$, ***$p < 0.005$ Dunnett's test. Error bars represent ± SEM, and $n \geq 12$.

(F) DON concentration of infected spikelet tissue 7 and 14 dpi with GFP-tagged *F. graminearum* strains as indicated. Water-inoculated spikelets served as control. **$p < 0.01$ Dunnett's test. Error bars represent ± SEM , and $n = 3$. nd, not detectable.

Figure 3. Non-cellulosic monosaccharide composition of *B. distachyon* spikelets after *F. graminearum* infection.

Cell wall extracts from infected spikelets at **(A)** 7 d post-inoculation (dpi) and **(B)** 14 dpi with the GFP-tagged *F. graminearum* strains wt-GFP, Δ*tri5*-GFP, Δ*flg1*-GFP, and Δ*gpmk1*-GFP were used. Water-inoculated spikelets served as control. Non-cellulosic monosaccharide composition determined by HPAEC-PAD (high-performance anion exchange chromatography with pulsed amperometric detection). a,b: $p < 0.05$ Dunnett's test. Error bars represent ± SEM , and $n = 3$. Ara, L-arabinose; Gal, D-galactose; Glu, D–glucose; Xyl, D-xylose.

Figure 4. DON-induced cell wall changes in *B. distachyon* spikelets.

A single floret of a spikelet was point-inoculated with DON solutions at concentrations ranging from 1 ppb to 500 ppm. Spikelets inoculated with water and *F. graminearum* strain wt-GFP served as control.

(A) Longitudinal spikelet section (left part of each panel) and isolated lemma (right part of each panel) of an inoculated floret 7 d after water and DON application at a concentration of 500 ppm. Red asterisk indicates point-inoculated floret. Scale bars = 2 mm.

(B) Non-cellulosic monosaccharide composition of cell wall extracts from spikelets treated with DON at indicated concentrations 7 d after application. a,b: $p < 0.05$ Dunnett's test. Error bars represent ± SEM, and $n = 3$. Ara, L-arabinose; Gal, D-galactose; Glu, D–glucose; Xyl, D-xylose.

Figure 5. DON-induced resistance to *F. graminearum* colonization of *B. distachyon* spikelets.

(A) Longitudinal section of spikelets infected with the wild-type *F. graminearum* strain wt-GFP to highlight disease phenotype 14 d post-inoculation (dpi). Spikelets were pretreated by spraying a DON solution (concentration: 1 ppm) and water as control 7 d before *F. graminearum* inoculation. Red asterisk indicates point-inoculated floret. Scale bar = 2 mm.

(B) Disease score of water- and DON-pretreated spikelets 14 dpi with *F. graminearum* wt-GFP. a,b: $p < 0.05$ Dunnett's test. Error bars represent ± SEM, and $n \geq 12$.

(C) Non-cellulosic monosaccharide composition of cell wall extracts from spikelets 7 d after spraying (0 dpi, time-point of *F. graminearum* inoculation) of DON or water as control (as described in (A)) and 14 dpi of the pretreated spikelets with *F. graminearum* wt-GFP. a,b,c: $p < 0.05$ Dunnett's test. Error bars represent ± SEM , and $n = 3$. Ara, L-arabinose; Gal, D-galactose; Glu, D–glucose; Xyl, D-xylose.

(D) Expression analysis of pathogen- and DON-inducible genes in DON- and water-pretreated *B. distachyon* spikelets at the time-point of *F. graminearum* wt-GFP inoculation (0 dpi) and 7 dpi. Water-sprayed, unchallenged spikelets served as control. a,b,c,d: $p < 0.05$ Dunnett's test. Error bars represent ± SEM , and $n = 3$. A repeat experiment gave similar results. *BdPR1.1*/*BdPR2*, pathogenesis related genes; *BdXET*, xyloglucan xyloglucosyl transferase; *BdUGT*, UDP-glycosyltransferase; *BdMAPKKK*, mitogen-activated protein kinase kinase kinase.